

## Millimeter Wave Imaging of Notches in Metal Specimens under Dielectric Coating Using Image Processing

Azadeh Noori Hoshyar<sup>1</sup>, Sergey Kharkovsky<sup>2</sup>, Bijan Samali<sup>3</sup> and Reza Zoughi<sup>4</sup>

<sup>1,2,3</sup> Centre for Infrastructure Engineering, SCEM, Western Sydney University, Australia

<sup>4</sup> Applied Microwave Nondestructive Testing Laboratory, ECE Department, Missouri University of Science and Technology, USA

**ABSTRACT:** Structural health monitoring is one of the main concerns in infrastructure engineering since it focuses on evaluating the life span of structures and detection of defects and damages, which may lead to sudden failure of structural components. This is why, in recent years, defect and damage detection and evaluation have received a wide attention among researchers. More specifically, a local structural health monitoring based on non-destructive testing techniques is an efficient approach to identify the defects and damages of structures in early stages to evaluate the remaining life span, improving safety and health of structures and increasing their serviceability. Therefore, the development and application of non-destructive testing and evaluation techniques including microwave and millimeter wave imaging of structures are very important. This paper presents the application of a relatively simple millimeter wave continuous wave reflectometer with an open-ended waveguide antenna and the developed image processing algorithms for the purpose of detection and evaluation of flaws such as cracks and notches on metal surface covered by dielectric coating such as rubber coating. It is shown that the original images based on measured data may not provide desired information, leading to developing the image processing algorithms to enhance the imaging results. Three different algorithm-based solutions are proposed and developed in this paper for automatic damage detection in infrastructures which complement the edge-based damage detection methods in hazardous scenarios. The proposed algorithms are based on Sobel, Canny, and fuzzy c-mean thresholding algorithms developed using Otsu's thresholding method to facilitate the structural damage identification. The notches in this paper represent damages in the metal plate such as cracks. The proposed algorithms have been compared together and with the traditional ones to investigate their performance and advantages. The proposed algorithms can successfully enhance the quality of images and visualize the damage on the metal surface under dielectric coating.

### 1 INTRODUCTION

Local structural health monitoring based on nondestructive testing (NDT) techniques play a crucial role for damage detection and evaluation in different structural components of infrastructure engineering. The patterns and the density of damage (e.g., crack) distributions disclose remarkable information to monitor the health of the system. In light of these important issues, imaging technology offers the cost-effective substitute way of inspection to identify

damages, Yan et al. (2002). Recently, there has been a wide interest in the use of microwave and millimeter wave imaging techniques for the purpose of NDT in civil infrastructure, Kharkovsky, et al. (2008), Kharkovsky, et al. (2012), Feng et al. (2013), Andrés et al. (2015), Adam et al. (2015) and Kharkovsky et al. (2016). Microwave and millimeter imaging techniques have a number of advantages. It is important that they are noncontact and one-sided techniques and can be applied for nondestructive testing and evaluation of non-transparent materials since their signals can penetrate inside dielectric materials and provide information of their entire structure. In common microwave and millimeter wave imaging techniques, the signals reflected from the specimen under test are recorded and used for detection of damage inside the specimen, Zoughi, (2000), Kharkovsky and Zoughi (2007), Ahanian et al. (2015). It can be called as local SHM for localization and evaluation of damages.

Different microwave and millimeter wave imaging systems have been used for NDT in infrastructure including relatively simple single-frequency reflectometers, and image generating algorithms, Zoughi, (2000), Kharkovsky and Zoughi (2007), Kharkovsky et al. (2008), Kharkovsky et al. (2009), and relatively complex wide-band reflectometers and image generating and processing algorithms such as synthetic aperture radar (SAR) one, Kharkovsky et al. (2012), Moosazadeh et al. (2016).

The detection and evaluation of cracks on the surface of metal are one of well-developed applications of microwave and millimeter wave imaging techniques, Zoughi, (2000), Kharkovsky and Zoughi (2007), Zoughi and Kharkovsky, (2008), Kharkovsky et al. (2009). This application is still in demand due to at least two reasons: 1) metal fatigue or failure usually begins from the surface, and 2) surface of the metal maybe covered with dielectric coating and may still be detected by these techniques, Zoughi, (2000). Variety of dielectric coatings and the requirements of relatively simple microwave and millimeter imaging techniques may create challenges and one of the solutions can be the use of single-frequency reflectometers along with the development and application of advanced image processing algorithms. This approach has been used for microwave imaging of relatively simple construction foam based specimens, Hoshyar et al. (2015). In this paper it is extended to millimeter wave imaging of notches in metal specimens under dielectric coating.

Millimeter wave imaging of notches are accomplished by applying the proper image processing techniques to enhance and segment the damage areas on obtained images. The segmentation algorithms are generally extended based on similarity and can be categorized as; thresholding, Cheriet et al. (1998), template matching, Lalonde et al. (2001), region growing, Mat-Isa et al. (2002), edge detection, Paik et al. (1991), and clustering, Yang et al. (2008). These techniques have been widely applied in various areas of statistics and recently found crucial applications in civil engineering, Yuan-Sen et al. (2015), Chun et al. (2013). Valença et al. (2013) proposed an automatic monitoring system using photogrammetry and image processing techniques to determine the crack areas. A high-pass filter and Otsu's method followed by mathematical morphology are the main image processing techniques have been used to identify the cracks. The major drawback of their research was incorrect detection of cracks along the test. In the research work of Hutchinson et al. (2006), the combination of Canny edge detection algorithm and the wavelet transform is presented to evaluate the concrete damage. In another research, Oh et al. (2009), a crack detection system has been designed to extract cracks in the bridge substructures by employing the Canny detection algorithm which reached the good image segmentation results. Qader et al. (2003) performed a comparison study on crack detection in the bridge surface by employing the wavelet transform, Fourier transform, Sobel filter, and Canny filter. Cotič et al. (2013), proposed the fusion of GPR and thermographic phase data and

improving the visualization of defects in concrete using the fuzzy c-mean algorithm. In this paper, three different algorithm-based solutions are proposed and developed for automatic damage detection in infrastructures which complement the edge-based damage detection methods in hazardous scenarios. The proposed algorithms are based on Sobel, Canny, and fuzzy c-mean thresholding algorithms developed by the Otsu's thresholding method to facilitate the structural damage identification.

The rest of this paper is structured as follows: the measurement approach and specimens are presented in Section 2. In Section 3, the proposed image processing algorithms for damage detection are explained in detail. The results are demonstrated in Section 4, and Section 5 is assigned to conclusion.

## 2 MEASUREMENT APPROACH AND SPECIMENS

### 2.1 *Measurement Approach*

In this investigation, a flanged section of standard W-band waveguide was used as an open-ended waveguide antenna (OEWA). The OEWAs are robust, reliable, efficient and relatively simple antennas for crack detection, Zoughi (2000), Kharkovsky and Zoughi (2007), Zoughi and Kharkovsky, (2008). The measurement setup was similar to that which had been used and described in Kharkovsky et al. (2009). It consisted of a computerized imaging system including a millimeter-wave reflectometer with a single frequency oscillator, isolator, magic tee, detector, variable short and the OEWA, and a scanning mechanism providing a raster scan of the reflectometer over the sample under test. All measurements were conducted at 90 GHz at different distances between the OEWA and the surface of specimen (referred to as standoff distance). The OEWA irradiated the specimen under test and picked up the signal reflected from the specimen. This reflected signal was combined with the reference signal in the magic tee, the combined data was sent to the detector and the computer recorded its output voltage for every data point over a plane for each specimen was measured. Images of the specimen were generated using the data and the proposed image processing algorithms.

### 2.2 *Specimens*

To highlight the utility of the millimeter-wave reflectometer along with the proposed image processing approaches for imaging of cracks/notches on the metal surface under dielectric coating such as rubber layer, a few specimens were prepared and imaged. The results for one of them are presented here.

The specimen consisted of an aluminum plate with the dimensions of 150 mm by 60 mm by 10 mm covered by a rubber layer. Two notches were made on the surface of plate, both with length of 15 mm and depth of 1 mm but with width of 1 mm and 0.5 mm in notch 1 and notch 2, respectively as shown in Figure 1. Two scanned areas with dimensions of 40 mm by 20 mm and 100 mm by 40 mm include notch 1 and notches 1 and 2, respectively, as shown in Figure 1, and the step size (sampling) of 1 mm and 0.5 mm along the length and width of the notches, respectively, were used in this investigation.

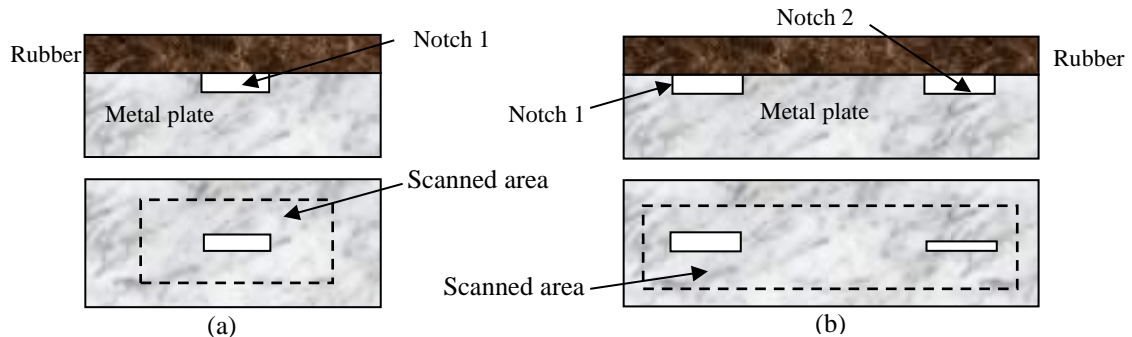


Figure 1. Cross-sectional side view (upper) and schematic of the top view without rubber layer (lower) of the parts of aluminum plate with (a) notch 1 and (b) notches 1 and 2.

### 3 THE PROPOSED IMAGE PROCESSING APPROACH

As the original images of the notches are not clear and have low resolution as will be shown below, three approaches have been investigated and run upon the same conditions to achieve the enhanced images and segmenting the area of defect. Since in image processing there is no single best approach, the algorithms should be dictated by the problems at hand, by the methods being used, and by the results required. To begin with, since the luminance of image is very crucial to distinguish the visual features, and the purpose here is to obtain the high level variations between intensities to detect the edges of defect, it would be optimal to convert the image into greyscale in which the minimum intensity value is equal to 0 and the maximum intensity value is equal to 255. Secondly, it is going to proceed the enhancement of raw images using the averaging filter and contrast enhancement technique. Enhancement in this case consists sharpening the image, while preserving as much as its gray tonality as possible. Firstly, it is required to generate and display the average filter. A rectangular averaging filter of size  $3 \times 3$  is considered. Since average filter is a separable filter, it can be implemented by dividing into two smaller filters. In this paper, firstly, the  $3 \times 1$  average filters is applied to the raw image and then the  $3 \times 1$  average filter proceeds the result. This process will result in less computational time. The new gray value of the corresponding pixel is calculated by taking the average of all nine values in the  $3 \times 1$  and  $3 \times 1$  masks. This process is followed by the grayscale transformation function to adjust the intensity. Since our images are of the class 'uint8', the function multiplies the values by 255 to specify the actual values in an image. To achieve the segmented notches from the background, the rest of this process is followed by three different methods.

In the first method, the directional gradients in x and y axis and gradient magnitude are calculated using Sobel's gradient operator. The edges of notch are returned at those points where the gradient of image is maximum. Therefore, the edges are achieved using the Sobel approximation to the derivative.

The second method uses the canny edge detection in its process. The gradient is calculated using the derivative of a Gaussian filter. It employs two thresholds and weak edges and local maxima of the gradient are considered as edges.

In the third method, the fuzzy c-mean thresholding algorithm has been improved by the effective selection of threshold value. The threshold value obtained by the Otsu's thresholding method is employed to improve the threshold value of fuzzy c-mean threshold value. The centre value of thresholds is considered as a desired value, which is confirmed in the results to be more likely to detect true edges. Edge ignores all edges that are not stronger than threshold value.

Figure 3 show the total scheme of these three algorithms and Figure 4 show the total scheme of comparison between the developed fuzzy c-mean thresholding algorithm and the traditional fuzzy c-mean thresholding algorithm.

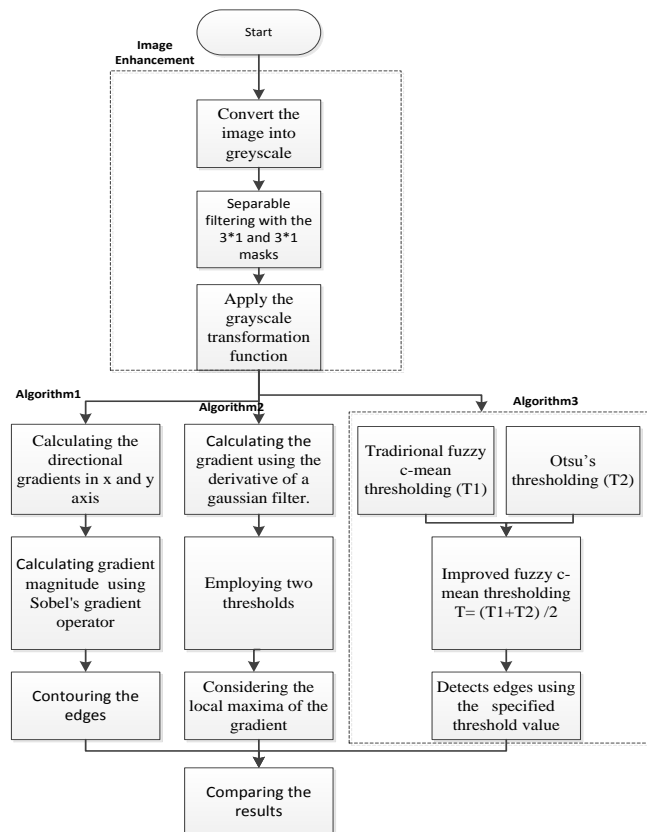


Figure 3. Total scheme of three algorithms.

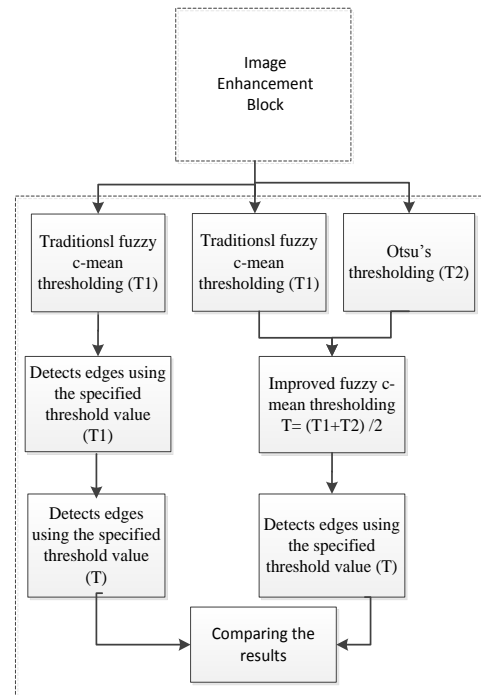


Figure 4. Total scheme of comparison between our proposed algorithm with traditional fuzzy c-mean thresholding algorithm.

#### 4 RESULTS

Figures 5 and 6 shows the images of notch 1 and notches 1 and 2, respectively, under 2-mm thick rubber layer obtained at standoff distance of 0.1 mm before and after performing the image enhancement block presented in Figure 3. As it is clearly seen from Figure 5(a) and 5(b), the original images are blurring, and also no information can be gained from images of notches under the 4-mm thick rubber layer as shown in Figures 5(c) and 6(a). By applying the image enhancement algorithm, the notches in the specimen are becoming clearly appeared as shown in Figures 5(a), 5(b) 5(c) and 6(b), which is considered as one of the goals of this investigation.

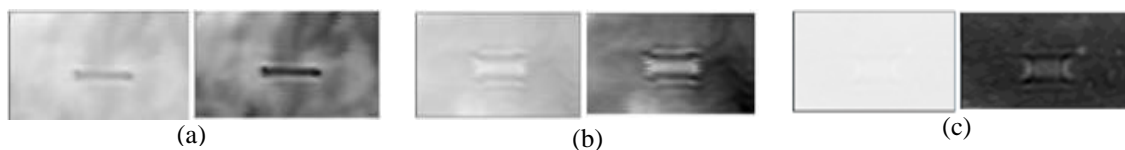


Figure 5. Original (left) and enhanced (right) images of notch 1 under the 2-mm thick rubber layer obtained at three standoff distances: (a) 0.1mm, (b) 0.25 mm and (c) 4 mm.



Figure 6. (a) Original and (b) enhanced images of notches 1 and 2 under the 4-mm thick rubber layer obtained at standoff distance of 0.1 mm.

The enhanced image of notch 1 (Figure 5(a)) were used to apply three image processing algorithms presented in Figure 3. Figures 7, 8 and 9 show the images of notch 1 before and after applying these algorithms. In Figures 7, the images obtained by algorithm (1) in Figure 3 are shown. The horizontal and vertical gradients along with the gradient magnitude using Sobel's gradient operator are calculated to segment the enhanced image.

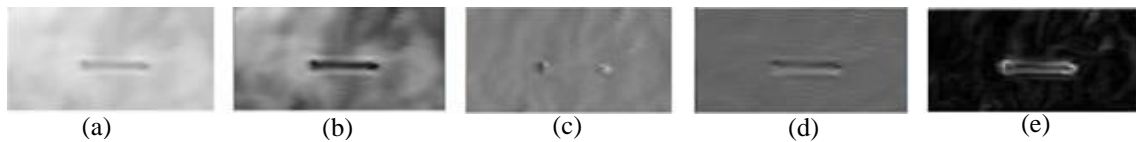


Figure 7. Images of notch 1 under the 2-mm thick rubber layer obtained at standoff distance of 0.1 mm: (a) original and after (b) average filtering, (c) gradient filtering in x direction ( $G_x$ ), (d) gradient filtering in y direction ( $G_y$ ) and e) gradient magnitude with Sobel method,  $|G| = \sqrt{G_x^2 + G_y^2}$ .

Figures 8 shows the images of notch 1 obtained with algorithm (2) (c.f. Figure 3). The Canny edge detection algorithm is applied to segment the enhanced image. The notch edges are detected by calculating the local maxima of the gradient of the image.

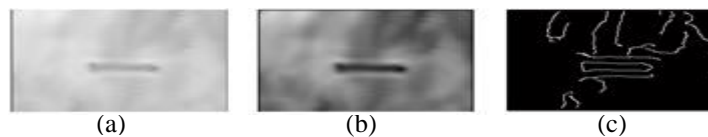


Figure 8. Images of notch 1 under the 2-mm thick rubber layer: (a) original and after (b) average filtering, (c) canny edge detection algorithm obtained at standoff distance of 0.1 mm.

Figure 9 shows the images of notch 1 obtained with algorithm (3) (c.f. Figure 3). The developed fuzzy c-mean thresholding algorithm is applied to segment the image. The obtained threshold value is 3.4E-01, while it is 1.7E-01 and 2.4E-01, respectively, for Otsu's thresholding method and traditional fuzzy-c-mean thresholding algorithm.

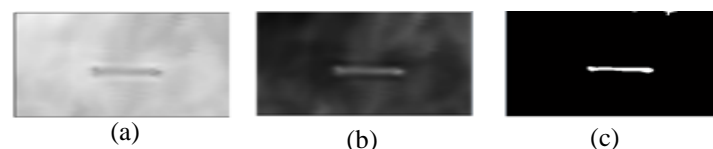


Figure 9. Images of notch 1 under the 2-mm thick rubber layer obtained at standoff distance of 0.1 mm.: (a) original and after (b) average filtering and (c) thresholding by the developed fuzzy c-mean thresholding algorithm.

Figure 10 show the comparison of segmented images of notch 1 obtained with algorithm (1), algorithm (2), and algorithm (3). According to the segmented images, our developed fuzzy c-mean thresholding algorithm outperforms the other two algorithms. It is obvious from Figure 10 (c), that the true edges which have been detected by the developed fuzzy c-mean thresholding algorithm are more accurate with less noise, while Figures 10 (a) and (b) include redundant edges and noise which are representing the segmentation error.

Figure 11 shows the comparison of developed fuzzy c-mean thresholding algorithm, traditional fuzzy c-mean thresholding algorithm and Otsu's thresholding algorithm. The results of this comparison show the better performance was obtained with improved fuzzy c-mean thresholding algorithm.

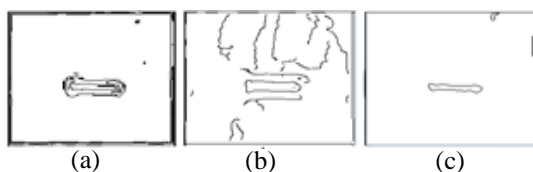


Figure 10. Notch edge detection obtained with the a) gradient magnitude using Sobel's gradient, b) Canny edge detection algorithm and c) developed fuzzy c-mean thresholding algorithm.

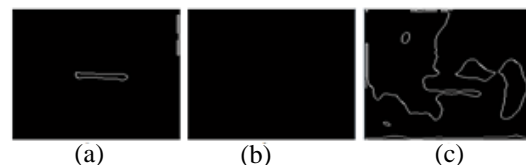


Figure 11. Notch edge detection obtained with a) the developed fuzzy c-mean thresholding algorithm, b) traditional fuzzy c-mean thresholding algorithm and c) Otsu's thresholding algorithm.

Imaging results confirm that the developed algorithm can identify the notch edges while eliminate the noises on the target region. It is shown that the algorithm provides the image with pure texture and strong edges.

## 5 CONCLUSION

In this paper, the image processing algorithms were investigated and developed to enhance the images of notches in metal specimens under rubber coating obtained by the millimeter wave reflectometer with an open-ended waveguide antenna at 90 GHz. The processed results are compared to show the effectiveness of developed algorithm in providing the enhanced and pure texture of defected region. It was shown that the developed fuzzy c-mean thresholding algorithm outperforms the traditional and other two algorithms, and can identify and manifest the notches before it become visible to the naked eye.

## REFERENCES

- Adam B., Aled J. and Sam K., 2015, "Microwave processing of cement and concrete materials – towards an industrial reality", *Cement and Concrete Research*, 68, 112–123.
- Ahanian I., Sadeghi S.H.H. and Moini R., 2015, "An array waveguide probe for detection, location and sizing of surface cracks in metals", *NDT&E International*, 70, 38–40.
- Andrés F., Castro M. and Valcuende B.V., 2015, "Using microwave near-field reflection measurements as nondestructive test to determine water penetration of concrete", *NDT&E International*, 26–32.
- Cheriet M., Said J. N. and Suen C. Y., 1998, "A recursive thresholding technique for image segmentation", *IEEE Transactions on Image Processing*, 7(6): 918- 921.
- Chun L., Chao-Sheng T., Bin S. and Wen-Bin S., 2013, "Automatic quantification of crack patterns by image processing", *Computers & Geosciences*, 57, 77-80.

- Cotič P., Niederleithinger E., Bosiljkov V., Jagličić Z., 2013, "NDT data fusion for the enhancement of defect visualization in concrete", *Key Engineering Materials*, 569, 175-182.
- Feng M.Q., Roqueta G. and Jofre L., 2013, "Non-destructive evaluation (NDE) of composites: microwave techniques", *Non-Destructive Evaluation (NDE) of Polymer Matrix Composites*, 574-616.
- Hoshyar A.N., Kharkovsky S. and Samali B., 2015, "Microwave imaging of composite materials using image processing", *International Symposium on Antennas and Propagation (ISAP2015)*, 465-468.
- Hutchinson T.C., Chen Z.Q., 2006, "Improved image analysis for evaluating concrete damage", *J. Comput. Civ. Eng.*, 20(3):210-216.
- Kharkovsky S. and Zoughi R., 2007, "Microwave and millimetre wave nondestructive testing and evaluation: Overview and recent advances", *IEEE Instrumentation & Measurement Magazine*, 10(2): 26-38.
- Kharkovsky S., Ryley A.C., Stephen V. and Zoughi R., 2008, "Dual-polarized near-field microwave reflectometer for noninvasive inspection of carbon fiber reinforced polymer-strengthened structures," *IEEE Transactions on Instrumentation and Measurement*, 57(1):168-175.
- Kharkovsky S., Ghasr M.T. and Zoughi R., 2009, "Near-field millimeter wave imaging of exposed and covered fatigue cracks," *IEEE Transactions on Instrumentation and Measurement*, 58(7): 2367-2370.
- Kharkovsky S., Case J. T., Ghasr M.T., Zoughi R., Bae S. and Belarbi A., 2012, "Application of microwave 3D SAR imaging technique for evaluation of corrosion in steel rebars embedded in cement-based structures," *In Review of Progress in Quantitative Nondestructive Evaluation*, American Institute of Physics, Melville, NY.
- Kharkovsky S., Giri P. and Samali B., 2016, "Non-contact inspection of construction materials using 3-axis multifunctional imaging system with microwave and laser sensing techniques," *IEEE Instrumentation and Measurement Magazine*, 19(2): 6 – 12.
- Lalonde M., Beaulieu M., and Gagnon L., 2001 "Fast and robust optic disc detection using pyramidal decomposition and Hausdorff-based template matching," *IEEE Transactions on Medical Imaging*, 21(11): 1193-1200.
- Mat-Isa N. A., Mashor M. Y., and Othman N. H., "Automatic seed based region growing for pap smear image segmentation," in Kuala Lumpur, *International Conference on Biomedical Engineering*, 2002.
- Moosazadeh M., Kharkovsky S. and Case J.T., 2016, "Microwave and millimetre wave antipodal Vivaldi antenna with trapezoid-shaped dielectric lens for high-range resolution imaging," *IET Microwaves, Antennas & Propagation*, 10(3): 301-309.
- Oh J.K., Jang G. and Oh S., 2009, "Bridge inspection robot system with machine vision", *Autom. Constr.*, 18(7): 929-941.
- Paik J. K., Park Y. C., and Park S. W., 1991, "An edge detection approach to digital image stabilization based on tri-state adaptive linear neurons," *IEEE Transactions on Consumer Electronics*, 37, 521-530.
- Yang X., Weidong Z., Yufei C., and Xin F., 2008, "Image segmentation with a fuzzy clustering algorithm based on Ant-Tree," *Signal Processing*, 88(10): 2453- 2462.
- Qader, O., Abu d., and Kelly M., 2003, "Analysis of edge-detection techniques for crack identification in bridges" *J. Comput. Civ. Eng.*, 17(4): 255-263.
- Valença J., Dias-da-Costa D., Júlio E., Araújo H. and Costa H., 2013, "Automatic crack monitoring using photogrammetry and image processing", *Measurement*, 46, 433-441.
- Yan, A., Wu, K. and Zhang, X., 2002, "A quantitative study on the surface crack pattern of concrete with high content of steel fiber". *Cement and Concrete Research*, 32(9): 1371-1375.
- Yang X., Weidong Z., Yufei C. and Xin F., 2008, "Image segmentation with a fuzzy clustering algorithm based on Ant-Tree," *Signal Processing*, 88(10): 2453- 2462.
- Yuan-Sen Y., Chung-Ming Y. and Chang-Wei H., 2015, "Thin crack observation in a reinforced concrete bridge pier test using image processing and analysis", *Advances in Engineering Software*, 83, 99-108.
- Zoughi, R., 2000, "Microwave non-destructive testing and evaluation", *Kluwer Academic Publishers*, Dordrecht, Netherlands.
- Zoughi R. and Kharkovsky S., 2008, "Microwave and millimeter wave sensors for crack detection," *Fatigue & Fracture of Engineering Materials & Structures*, 31(8): 695-713.